The Astrophysical Journal, 653:1194–1202, 2006 December 20

HYPERVELOCITY STARS: PREDICTING THE SPECTRUM OF EJECTION VELOCITIES

Benjamin C. Bromley
Department of Physics, University of Utah, 115 S 1400 E, Room 201, Salt Lake City, UT 84112;
bromley@physics.utah.edu

Scott J. Kenyon and Margaret J. Geller
Smithsonian Astrophysical Observatory, 60 Garden Street, Cambridge, MA 02138;
skenyon@cfa.harvard.edu, mgeller@cfa.harvard.edu

Elliott Barcikowski
Department of Physics, University of Utah, 115 S 1400 E, Room 201,
Salt Lake City, UT 84112; elliottb@physics.utah.edu

and

Warren R. Brown and Michael J. Kurtz
Smithsonian Astrophysical Observatory, 60 Garden Street, Cambridge, MA 02138;
wbrown@cfa.harvard.edu, mkurtz@cfa.harvard.edu
Received 2006 July 5; accepted 2006 August 4

ABSTRACT

The disruption of binary stars by the tidal field of the black hole in the Galactic center can produce the hypervelocity stars observed in the halo. We use numerical models to simulate the full spectrum of observable velocities of stars ejected into the halo by this binary disruption process. Our models include a range of parameters for binaries with 3–4 $M_\odot$ primaries, consideration of radial orbits of the ejected stars through an approximate mass distribution for the Galaxy, and the impact of stellar lifetimes. We calculate the spectrum of ejection velocities and reproduce previous results for the mean ejection velocity at the Galactic center. The model predicts that the full population of ejected stars includes both the hypervelocity stars with velocities large enough to escape from the Galaxy and a comparable number of ejected, but bound, stars of the same stellar type. The predicted median speeds of the population of ejected stars as a function of distance in the halo are consistent with current observations. Combining the model with the data also shows that interesting constraints on the properties of binaries in the Galactic center and on the mass distribution in the Galaxy can be obtained even with modest samples of ejected stars.

Subject headings: binaries: general — Galaxy: center — Galaxy: halo — stellar dynamics

1. INTRODUCTION

Hypervelocity stars (HVSs) are objects moving with speeds sufficient to escape the gravitational influence of the Galaxy. Hills (1988) predicted their existence, and Brown et al. (2005) discovered the first HVS in a survey of blue stars within the Galactic halo. We now know of seven HVSs (Edelmann et al. 2005; Hirsch et al. 2005; Brown et al. 2006a, 2006b). One HVS is a subdwarf O star at a distance of ~20 kpc from the Galactic center (Hirsch et al. 2005). The other HVSs are probably B-type main-sequence stars with galactocentric distances of 50–100 kpc. The five late-B stars in this group have masses $m \sim 3$–$4\ M_\odot$ (Brown et al. 2006a, 2006b). The early B-type HVS is more massive, $m \sim 8\ M_\odot$ (Edelmann et al. 2005).

Only two proposed models plausibly explain the origin of the observed population of Galactic HVSs. In the single black hole model, a binary system strays too close to Sgr A*, the 3.5 million solar-mass black hole in the Galactic center (Hills 1988, 1992; Yu & Tremaine 2003; Gould & Quillen 2003). This encounter tears the binary apart, leading to the capture of one star and the high-speed ejection of its partner (Hills 1988). For typical ejection velocities of ~2000 km s^{-1}, the HVS can reach galactocentric distances of ~50 kpc in ~25 Myr (Hills 1988, 1992; Yu & Tremaine 2003; Gould & Quillen 2003; Brown et al. 2006b; Perets et al. 2006), roughly the lifetime of a 9 $M_\odot$ star (Schaller et al. 1992; Schaerer et al. 1993).

Other HVS models involve three-body interactions between a single star and a binary black hole. Random encounters between stars near the Galactic center and a binary black hole can lead to an HVS with a typical ejection velocity of ~2000 km s^{-1} (Quinlan 1996; Yu 2002; Yu & Tremaine 2003; Gualandris et al. 2005; Sesana et al. 2006). Alternatively, the inspiral of an intermediate-mass black hole with $m \sim 10^3$–$10^4\ M_\odot$ can eject stars from the Galactic center (e.g., Hansen & Milosavljević 2003). Some of these encounters will produce HVSs with ejection velocities of ~2000 km s^{-1} (Levin et al. 2005; Baumgardt et al. 2006; Sesana et al. 2006). Although binary black holes with circular orbits and inspiraling black holes produce roughly isotropic distributions of HVSs on the sky, eccentric binary black holes can produce anisotropic space distributions of HVSs (Holley-Bockelmann et al. 2005; Baumgardt et al. 2006; Sesana et al. 2006).

Here we use numerical simulations to predict the distribution of observable radial velocities of HVSs ejected by a single black hole at the Galactic center. Our results identify a new population of ejected stars of the same stellar type as the HVSs, but more slowly moving. Ongoing halo surveys (Brown et al. 2006b) show evidence of this population. The distribution of observable radial velocities among these stars may yield information about the nature of the progenitor binaries and can serve as a probe of the distribution of mass throughout the Galaxy. Even the small number of known HVSs can constrain the distribution of mass in the

Milky Way (see also Gnedin et al. 2005). We describe the basic model and the numerical simulations in § 2, compare the numerical results with observations in § 3, and conclude with a discussion and summary in § 4.

2. THE MODEL

2.1. *Overview*

The goal of this study is to develop methods for predicting the observable velocity distribution of HVSs in the Galactic halo. We derive velocity distributions appropriate for the single black hole at the Galactic center; we do not consider models for ejections from binary black holes (e.g., Yu & Tremaine 2003; Gualandris et al. 2005; Levin et al. 2005). Previous analytical and numerical analyses have concentrated on the production of HVSs from the interactions of binary stars with the massive black hole in the Galactic center (Hills 1988, 1992; Yu & Tremaine 2003; Gould & Quillen 2003; Perets et al. 2006). However, the observable distribution of HVSs also depends on the mass distribution in the Galactic center and on the gravitational potential of the Milky Way (e.g., Gnedin et al. 2005). Here we adopt a simple prescription for the Galactic mass distribution, integrate the orbits of stars ejected from the Galactic center, and derive a first approximation to the full observable phase-space distribution of ejected stars on radial orbits in the halo. Comparisons between observations of halo stars with the model predictions then yield constraints on the mass function of binaries in the Galactic center and the Galactic potential.

We simulate the ejection of stars from the Galactic center in three steps. Following Hills (1988), we first integrate orbits of binary stars passing by Sgr A* to quantify ejection probabilities and velocities. Then we use a Monte Carlo code based on semianalytical approximations for rapid generation of simulated catalogs of ejected stars in the Galactic center. Finally, we integrate the orbits of these stars in the Galactic potential to derive how they populate the Galaxy's halo. To generate observable samples, the simulation incorporates the stellar main-sequence lifetime from published stellar evolution calculations. In this first study, we focus on binaries with the full range of possible initial separations and with primary star masses of $3-4\,M_\odot$, corresponding to halo B stars targeted in ongoing radial velocity surveys (Brown et al. 2006a, 2006b).

2.2. *Simulations of Binary Interactions with the Central Black Hole*

To follow the evolution of a binary as it interacts with a massive black hole, we use a sixth-order, symplectic integrator (Yoshida 1990). Bromley & Kenyon (2006) describe tests of this code in the context of a simulation of planet formation (see also Kenyon & Bromley 2006). For the three-body simulations here, the algorithm restricts energy errors to less than 1 part in 10^9. Our numerical trials start with randomly oriented binary stars, launched toward the black hole from a distance of several thousand AU, much larger than the binary separation (generally less than a few AU). As in Hills (1988), we assume that the initial approach speed of the binary center of mass is 250 km s^{-1} and that the binary star orbit has negligible eccentricity. Variations in the initial approach speed have little impact on the results. Although the binary eccentricity can affect the outcome of an ejection event, stars in eccentric binaries spend most of their time at separations larger than the orbital semimajor axis. Thus, results for eccentric binaries generally mimic results for circular binaries with appropriately larger semimajor axes. Table 1 lists the ranges of other input parameters used in these calculations.

TABLE 1
MODEL PARAMETERS

Parameter	Symbol	Value or Range
Sgr A* mass	$M_\bullet$	$3.5 \times 10^6\ M_\odot$
Primary mass	m_1	$3-4\ M_\odot$
Secondary mass	m_2	$0.5-4\ M_\odot$
Binary semimajor axis	$a_{\rm bin}$	0.05–4 AU
Closest approach distance	$R_{\rm min}$	~1–700 AU
Galactic density index[a]	α	1.8–2.5
Galactic "core" radius	a_c	1–33 AU
Galactic central density[b]	ρ_0	6270–162,000 $M_\odot$ pc^{-3}

[a] The parameters α, a_c, and ρ_0 are defined in eq. (6).
[b] These values do not include the mass of Sgr A*.

Our simulations reproduce published numerical results, and they are consistent with analytical expectations for the production of HVSs (Hills 1988, 1992; Yu & Tremaine 2003; Gould & Quillen 2003). The high-speed ejection of a binary member from an encounter with a massive black hole depends on the binary's semimajor axis $a_{\rm bin}$, the closest approach distance between the binary and the black hole $R_{\rm min}$, and the masses of the three bodies—$M_\bullet$ is the black hole mass, and m_1 and m_2 are the masses of the primary and secondary binary partners, respectively. For encounters that produce an ejected star, our numerical simulations yield (see also Hills 1988)

$$v_{\rm ej} = 1760 \left(\frac{a_{\rm bin}}{0.1\ {\rm AU}}\right)^{-1/2} \left(\frac{m_1+m_2}{2\ M_\odot}\right)^{1/3} \times \left(\frac{M_\bullet}{3.5\times10^6\ M_\odot}\right)^{1/6} f_R\ {\rm km\ s^{-1}}, \quad (1)$$

where the factor f_R is of order unity and serves to tune the ejection speed in accord with numerical simulations (as in Fig. 3 of Hills 1988). To approximate the Hills results, we derive a quintic polynomial fit for f_R

$$f_R = 0.774 + (0.0204 + \{-6.23\times10^{-4} + [7.62\times10^{-6} + (-4.24\times10^{-8} + 8.62\times10^{-11}D)D]D\}D)D,$$

where the Hills parameter D is defined in equation (3) below. For an unequal-mass binary, the ejection speeds of the primary and secondary are

$$v_1 = v_{\rm ej}\left(\frac{2m_2}{m_1+m_2}\right)^{1/2}, \quad v_2 = v_{\rm ej}\left(\frac{2m_1}{m_1+m_2}\right)^{1/2}, \quad (2)$$

respectively.

We confirm that both stars are rarely ejected during an encounter (Hills 1988). Furthermore, for the types of binary orbits and mass ranges that we consider the primary and secondary have an approximately equal chance of ejection. The key factors in the ejection are the orbital phase and orientation of the orbital plane when the binary comes under the grip of the black hole's tidal field. Our simulations suggest that if a binary is disrupted, then the star on the orbit closest to the black hole tends to be captured; its partner is ejected. When there is a significant difference between primary and secondary masses, the primary is more likely to be ejected. We can understand this preference in the limit of a very large mass ratio, where the primary follows its unbound Keplerian orbit about the black hole and the secondary may be captured. However, for the mass ratios and orbital configurations

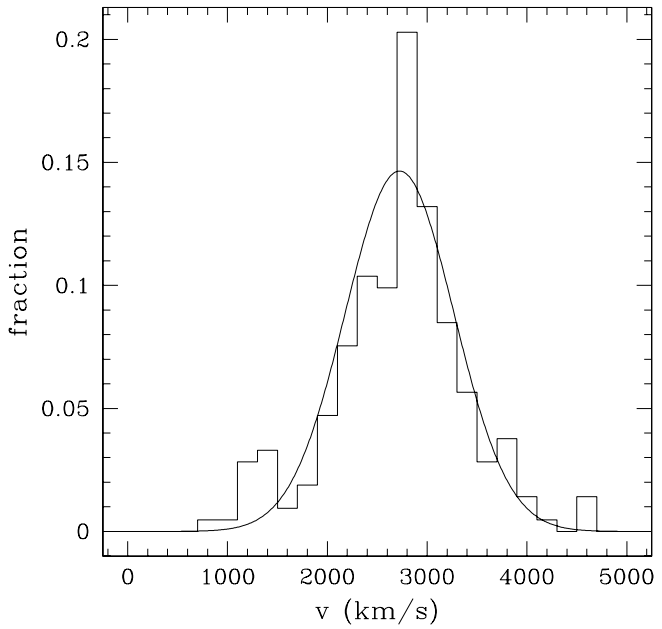

FIG. 1.—Distribution of ejection speeds from a binary with a 4 $M_\odot$ primary star, just after encountering a black hole with a mass of $3.5 \times 10^6\ M_\odot$. The original binary has a semimajor axis of 0.1 AU, and its center of mass is targeted to reach a minimum distance of 5 AU from the black hole.

that produce the ejection speeds of interest here our simulations suggest that we may neglect any preference in the ejection of the primary star.

The ejection speeds in equations (1) and (2) represent averages and are the theoretical speeds at infinite distance from the black hole in the absence of other gravitational sources. Figure 1 illustrates our calculated distribution of ejection speeds for equal-mass binaries after encountering Sgr A*, with $M_\bullet = 3.5 \times 10^6\ M_\odot$. The distribution has a pronounced peak at $\sim$2800 km s^{-1} and broad wings extending to $\sim$1000 and $\sim$4000 km s^{-1}. The solid line in Figure 1 shows that a Gaussian with $v_{\rm avg} \sim 2600$ km s^{-1}, $\sigma_v \sim 0.2$, and $v_{\rm avg} \sim 500$ km s^{-1} provides a reasonable characterization of the numerical results. Repeated trials for a wide range of binary configurations indicate that the Gaussian model generally gives an adequate description of the ejection speed distribution. We use this simple Gaussian model as input to the Monte Carlo simulations of the predicted distribution of speeds as a function of distance from the Galactic center. Our simulations confirm that the final distribution of ejected stars in the halo is insensitive to our particular choice of σ_v within reasonable limits.

The shape of the velocity distribution in Figure 1 reflects the detailed dependence of an ejection event on the orbital phase and orientation of the binary orbit relative to the black hole. We speculate that the extended tails of the distribution correspond to infrequent encounters in which the binary angular momentum is either strongly aligned or counteraligned with its center-of-mass angular momentum about the black hole. Otherwise, encounters yield velocities near the mean, causing a peak in the distribution near $v_{\rm avg}$. A study of a large ensemble of simulations may confirm this speculation and is beyond the scope of this initial study.

Given values of $a_{\rm bin}$ and $R_{\rm min}$, we derive the probability that a particular interaction leads to the ejection of a star. Following Hills (1988), we calculate a dimensionless quantity,

$$D = \left(\frac{R_{\rm min}}{a_{\rm bin}}\right)\left[\frac{2M_\bullet}{10^6(m_1+m_2)}\right]^{-1/3}, \qquad (3)$$

and derive the probability of an ejection as

$$P_{\rm ej} \approx 1 - D/175 \qquad (4)$$

for $0 \le D \le 175$. For $D > 175$, $R_{\rm min} \gg a_{\rm bin}$, and the binary does not get close enough to the black hole for an ejection. Thus, $P_{\rm ej}$ is zero in this case.

Our treatment of the ejection probability does not account for the possibility that a black hole–binary encounter will lead to a collision between the binary partners (Yu & Tremaine 2003; Ginsburg & Loeb 2006). Our simulations suggest that stellar collisions may be important for small values of $a_{\rm bin}$, but only at the O (10%) level. Furthermore, there is enough uncertainty in the possible outcome of such high-speed collisions, including rapidly rotating ejected stars or mergers (Ginsburg & Loeb 2006), that we do not consider their effect in this work. Instead we note that equation (4) may modestly overestimate the ejection probability in some cases.

Next, we calculate the broader distribution of ejection velocities that arise from encounters with a range of astrophysically relevant $a_{\rm bin}$ and $R_{\rm min}$ values. Surveys of large samples of binary systems with solar-type primary stars (e.g., Abt 1983; Heacox 1998) suggest that the probability density function for binary semimajor axes is roughly

$$p(a_{\rm bin})da_{\rm bin} \sim da_{\rm bin}/a_{\rm bin} \qquad (5)$$

for $a_{\rm bin} \sim 10^{-2}$–10^3 AU. Duquennoy & Mayor (1991) favor a Gaussian distribution in log P, where P is the orbital period. Here we adopt equation (5), which yields an equal number of objects in equally spaced logarithmic bins of the semimajor axis and is consistent with the distribution of $a_{\rm bin}$ derived from observations of smaller samples of binaries with O-type and B-type primary stars (Garmany et al. 1980; Kobulnicky et al. 2006). The probability density function of closest approach distances to Sgr A* varies linearly with $R_{\rm min}$, as a result of gravitational focusing (Hills 1988). With these probabilities, we use a Monte Carlo code to draw samples of $a_{\rm bin}$ and $R_{\rm min}$. We reject some fraction of samples according to equation (4) and feed the rest into equations (1) and (2) to derive average ejection speeds. A normally distributed random-number generator then provides ejection speeds with a 20% dispersion about the mean (eq. [1]). Thus, we produce catalogs of ejection events for specific binary masses and construct distributions of ejection speeds.

Unlike previous studies of ejected stars from the Galactic center, which were focused on HVSs, we admit wide ranges of $a_{\rm bin}$ and $R_{\rm min}$ to consider ejection events that would not necessarily yield stars capable of escaping the Galaxy. For the binary semimajor axis, we choose 0.05 AU $\le a_{\rm bin} \le$ 4 AU; the lower limit is suggested by the physical radius of the 4 $M_\odot$ primary (about half this length); the upper limit arises because we are interested in stars with sufficient ejection speeds to populate the Galactic halo beyond 10 kpc (cf. eq. [1]). Once we set the maximum $a_{\rm bin}$ value, equation (4) gives the maximum value of $R_{\rm min}$ that could result in a nonzero ejection probability.

The semianalytical approximations in equations (1)–(5) encode the underlying physics of ejections from the Galactic center. The Hills parameter D and the expression for the ejection probability in equation (4) are statements that the ability of Sgr A* to disrupt a binary depends most strongly on the ratio between the orbital separation and the closest approach distance; a tight binary is hard to disrupt when it does not get close to the black hole. However, once a binary is disrupted, the speed of the ejected star comes mainly from the kinetic energy available to the star from its binary

orbit, which scales as $1/a_{\rm bin}$ (eq. [1]). Finally, a broad distribution of ejection speeds arises from the interplay between binary separation and ejection probability. For example, a small binary separation—which can yield a high-speed ejection—is more likely than a large $a_{\rm bin}$, yet it has a low probability of producing an ejection for typical values of $R_{\rm min}$ (eq. [5]). Conversely, a large binary separation—which leads to a low-velocity ejection—is not common; however, should a system with large $a_{\rm bin}$ encounter Sgr A*, then an ejection event is highly likely. Within realistic ranges of $a_{\rm bin}$ and $R_{\rm min}$, ejection speeds can vary widely.

2.3. *The Galactic Potential and the Observed Velocity Spectrum*

To construct simulated catalogs of ejected stars that are relevant to HVSs searches in the Galactic halo, we next consider the effect of the Galactic potential. A simple parameterization of the distribution of mass in the Galaxy is

$$\rho(r) = \frac{\rho_0}{1 + (r/a_c)^{\alpha}}, \tag{6}$$

where r is the distance to the Galactic center, ρ_0 is the central density, a_c is a "core radius," and the index α is around 2 (Binney & Tremaine 1987, p. 601). Unless otherwise specified, we set $\rho_0 = 1.27 \times 10^4\ M_\odot\ {\rm pc}^{-3}$, $a_c = 8$ pc, and $\alpha = 2$; these choices give a mass within 10 pc of the Galactic center of $\sim 3 \times 10^7\ M_\odot$, as inferred from stellar kinematics in the region of Sgr A* (Eckart & Genzel 1997; Schödel et al. 2003; Ghez et al. 2005), and a circular rotation speed of 220 km s^{-1} in the solar neighborhood (Hogg et al. 2005).

To produce simulated surveys, we view the Galactic center as a fountain of ejected stars, spewing out at a steady rate. We focus on primary stars of 3–4 $M_\odot$, because these objects are the targets of ongoing B-star searches. Although B stars could be secondaries, we assume for this work that such binaries are relatively rare. Whether an ejected star becomes part of a simulated survey depends on (1) the spatial extent of the survey, (2) the main-sequence lifetime of the star, and (3) the time when the star was ejected relative to the present.

For the survey volume, we assign a 10 kpc inner radius and an outer radius of 90 kpc for 3 $M_\odot$ stars and 120 kpc for 4 $M_\odot$ stars, consistent with the selection in the survey of Brown et al. (2006a, 2006b). To derive the time since a star was ejected, we randomly generate an age, T, from a uniform distribution between zero and the main-sequence lifetime $t_{\rm ms}$, which is 350 Myr for 3 $M_\odot$ stars and 160 Myr for 4 $M_\odot$ stars (Schaller et al. 1992; Schaerer et al. 1993; Brown et al. 2006a). In doing so, we assume that the stars' pre–main-sequence phase is comparatively short, that the travel time between the parent binary and the black hole is also short, and that the scattering of the host binary toward Sgr A* is a random process that is equally likely at any time (see Yu & Tremaine [2003] and Perets et al. [2006] for descriptions of scattering mechanisms).

We use a second orbit integration code to calculate the radial trajectory of an ejected star as it travels through the potential generated by the mass density in equation (6). This code takes its input from the Monte Carlo ejection-speed generator, modified to account for the finite distance from the black hole. We start each ejected star's orbit near Sgr A*, at a distance where the Galactic mass model generates 5% of the black hole mass, typically within a parsec. The code integrates the orbit outward from this starting point, with a simple leapfrog (second-order symplectic) scheme to track radius and radial velocity as a function of time. It concurrently integrates the density (eq. [6]), using Simpson's rule, to derive values of the mass enclosed at each radius, a quantity needed for force evaluation. The integrator breaks off when the time reaches the star's randomly chosen age, T, or if the star falls back out of the survey volume toward the black hole. In this way, we build up simulated catalogs of ejected stars within the Galactic halo.

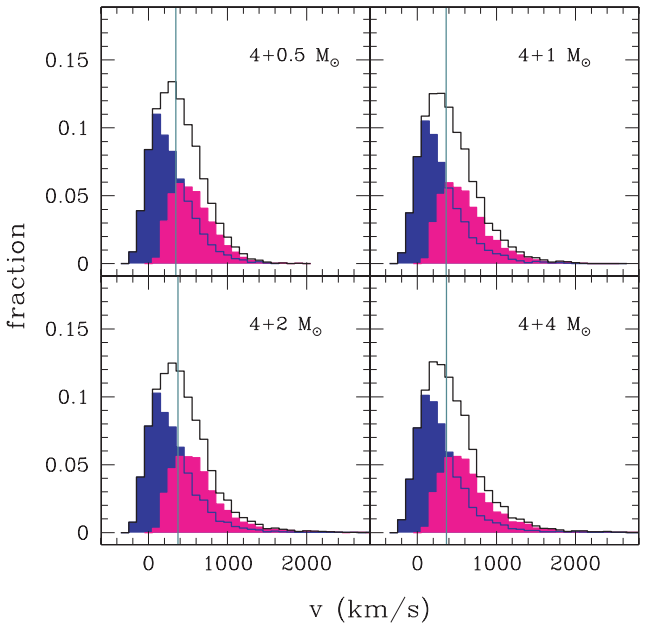

FIG. 2.—Distribution of observable speeds of ejected 4 $M_\odot$ primaries in the Galactic halo, as a function of the mass of the secondary. The secondary mass is indicated in each panel. The solid black histograms show the velocity distribution of all objects in a survey volume that extends from 10 to 80 kpc away from the Galactic center. The gray vertical lines locate the median velocity of each distribution. The blue histogram represents all objects inside a 40 kpc radius; the magenta histogram corresponds to objects outside this radius.

Figures 2–4 summarize the main results of these simulations. Figure 2 shows the observable velocity distribution as a function of secondary mass. The individual panels correspond to a 4 $M_\odot$ primary and secondary masses of 0.5, 1, 2, and 4 $M_\odot$, respectively. In all cases, the velocity distribution of stars in the range 10 kpc $< r <$ 120 kpc peaks near 300 km s^{-1}, with virtually no dependence on the mass of the secondary. Instead, the location of this peak is largely determined by the radial extent of the survey volume and the main-sequence lifetime. In the fountain picture, many of the slowly moving ejected stars can reach the inner halo ($r < 40$ kpc) within a time $t < t_{\rm ms}$, and some will even fall back toward the Galactic center. However, the ejection speeds must be faster just to reach larger radii within the stellar main-sequence lifetime. Thus, more distant regions of the halo tend to hold faster moving ejected stars. Figures 2–4 show this effect by comparing the velocity distribution peak for stars inside $r = 40$ kpc (*blue histograms*) with the distribution for stars located outside that radius (*magenta histograms*). The velocity distributions for nearby stars peak at $\sim$100 km s^{-1}; the peak moves to 400–500 km s^{-1} for more distant objects.

The overall velocity distribution of primary stars is insensitive to the mass of the secondary. In general, the stellar lifetime, combined with the Galactic potential, "filters" the distribution to admit slower speed ejected stars, which are prevalent regardless of the secondary mass. These slower speed ejecta live long enough to populate the inner Galactic halo in larger numbers compared to the high-velocity tail. At larger distances, only the high-velocity tail is observable, as a result of the short stellar lifetimes. The

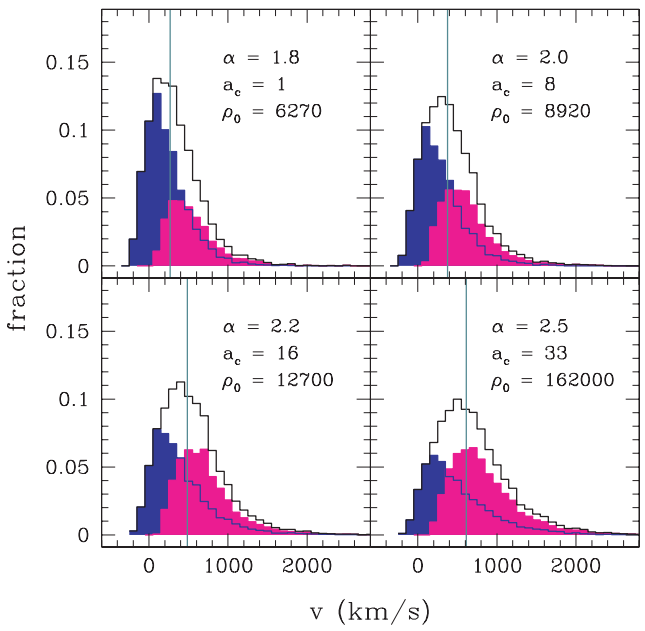

FIG. 3.—Same as the Fig. 2, but for the distribution of observable speeds of an ejected 4 $M_\odot$ primary with a 2 $M_\odot$ secondary, as a function of Galactic mass model. The model parameters, displayed in each panel, correspond to eq. (6).

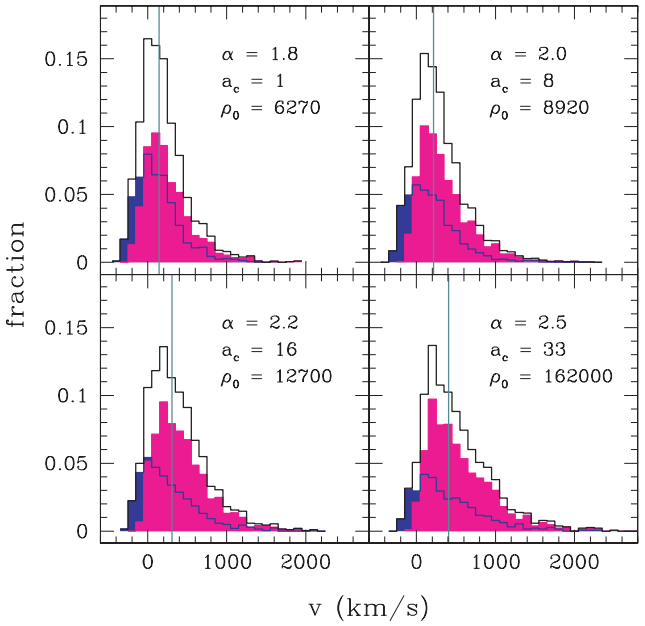

FIG. 4.—Similar to Fig. 3, but for the distribution of observable speeds of an ejected 3 $M_\odot$ primary with a 1.5 $M_\odot$ secondary, as a function of Galactic mass model. The survey volume in this case spans a radial extent of 10 kpc $< r <$ 90 kpc; the blue and magenta histograms correspond to populations inside and outside 30 kpc, respectively.

dependence of ejection velocity on secondary mass (eqs. [1]–[2]) is important only for the high-velocity tail of the observed velocity distribution. For example, the observation of a blue star with a speed in excess of 2000 km s^{-1} requires a secondary of at least 1 $M_\odot$ and statistically favors an even larger mass, because the likelihood of a hypervelocity ejection increases with the secondary mass.

Figure 3 illustrates the effect of the Galactic mass density profile on speeds of ejected 4 $M_\odot$ stars in the halo. Although the peak of the velocity distribution is relatively independent of the mass model, the median velocity is sensitive to model parameters. Changing the index α in equation (6) from 1.8 to 2.5 produces a significant variation in the median velocity of objects in the full survey volume (*black histograms in each panel*), from 270 km s^{-1} for $\alpha = 1.8$ to more than 600 km s^{-1} for $\alpha = 2.5$. The blue and magenta histograms show the sensitivity of the median to distance from the Galactic center. For halo stars beyond 40 kpc, the median velocity varies from 485 km s^{-1} for $\alpha = 1.8$ to 750 km s^{-1} for $\alpha = 2.5$.

Figure 4 shows similar results for binaries with a primary mass of 3 $M_\odot$ and secondary mass of 1.5 $M_\odot$. Compared to the 4 $M_\odot$ cases, the histograms shift to slower ejection speeds due to the lower luminosity and longer (350 Myr) lifetime of the lower mass stars. At the magnitude limit of optical surveys, stars with smaller optical luminosities have smaller distances; thus, these surveys are shallower for 3 $M_\odot$ stars than for 4 $M_\odot$ stars.

Table 2 summarizes the results for the median radial velocities in Figures 3 and 4. For each adopted α, the table lists the core radius (a_c) and central mass density (ρ_0) needed for a mass of $\sim 3 \times 10^7$ $M_\odot$ within 10 pc of the Galactic center and the median velocities for two samples of ejected stars for 3 and 4 $M_\odot$ primary stars. For 3 $M_\odot$ primaries, the full survey volume extends from 10 to 90 kpc; the halo volume extends from 30 to 90 kpc. For 4 $M_\odot$ primaries, the full survey volume extends from 10 to 120 kpc; the halo volume extends from 40 to 120 kpc.

In addition to producing smaller median observable speeds for lower mass stars, the main-sequence lifetimes set the maximum stellar mass for HVSs. For primary stars ejected with velocity $v_{\rm ej}$ from the Galactic center, Table 3 lists the maximum distance $d_{\rm max}$ the star can reach during its main-sequence lifetime. Because the travel time from the Galactic center to the Galactic halo, $t \propto m^{-1/3}$, has a much weaker mass dependence than the main-sequence lifetime, $t_{\rm ms} \propto m^{-2}$, massive stars ejected from the Galactic center cannot reach large galactocentric distances. Furthermore, high ejection speeds require a small binary semimajor axis (eq. [1]); larger, more massive stars have a larger minimum $a_{\rm bin}$ than smaller, less massive stars, based on an assessment of Roche lobe overflow (Eggleton 1983). Thus, less massive stars have maximum ejection velocities comparable to those of more massive stars—and hence larger $d_{\rm max}$, given enhanced stellar lifetimes. Based on the relative ejection velocities, stellar lifetimes, and the time needed for any star to reach the central black hole, we suggest that the maximum mass for an HVS in the outer halo is $\sim$12 $M_\odot$ (Table 3). With large surveys to greater depth, this mass limit may provide an observational test of these models.

Figures 2–4 show the breadth of speeds that ejected stars can have once they have traveled into the Galactic halo, from negative values—corresponding to infall—to hypervelocities. Clearly, HVSs have slower moving counterparts of the same stellar type that originated near the Galactic center and carry information about the physical process which led to their ejection. To illustrate this feature of the simulations in more detail, Figure 5 shows the fraction of escaping stars (with velocities exceeding the local escape velocity[1]) as a function of distance from the Galactic center. For 3 $M_\odot$ primaries, the fraction increases roughly linearly with radius and is almost 50% at $\sim$90 kpc, the limit of current surveys for these stars. The fraction of escaping stars is much larger for 4 $M_\odot$ primaries and is 100% at 80–120 kpc. In an ensemble of 3–4 $M_\odot$ ejected stars, the fraction of escaping stars is $\sim$50%, suggesting that observations should reveal roughly

[1] We calculate the escape velocity from the mass distribution in eq. (6) for a galaxy with an outer radius of 120 kpc. The results are nearly identical for outer radii of 250 kpc.

TABLE 2
MEDIAN OBSERVABLE SPEEDS OF EJECTED STARS AS A FUNCTION OF MASS MODEL

α[a]	a_c (pc)	ρ_0 ($M_\odot$ pc^{-3})	3 $M_\odot$[b] v_{med} (full)	3 $M_\odot$[b] v_{med} (halo)	4 $M_\odot$[c] v_{med} (full)	4 $M_\odot$[c] v_{med} (halo)
1.8.....	1	1.62×10^5	144	188	270	485
2.0.....	8	1.27×10^4	218	272	374	565
2.2.....	16	8920	306	370	484	648
2.5.....	33	6270	407	457	608	752

[a] The parameters α, a_c, and ρ_0 are defined in eq. (6).
[b] These columns list results for a primary mass of 3 $M_\odot$ and a secondary mass of 1.5 $M_\odot$. The radial extent of the full survey, v_{med} (full), is 10–90 kpc; the radial extent of the halo survey, v_{med} (halo), is 30–90 kpc. The listed values correspond to the median radial velocity of the ensemble of ejected stars.
[c] These columns list results for a primary mass of $4v_{med}$ and a secondary mass of $2v_{med}$. The radial extent of the full survey, v_{med} (full), is 10–120 kpc; the radial extent of the halo survey, v_{med} (halo), is 40–120 kpc. The listed values correspond to the median radial velocity of the ensemble of ejected stars.

comparable numbers of unbound HVSs and ejected, but bound, halo stars with lower observed radial velocities. To test this and other aspects of the calculation, we now compare our results with observed velocity distributions of stars in the Galactic halo.

3. COMPARING THE MODEL WITH OBSERVATIONS

The model for HVSs has several observable and testable consequences. To produce an observable ensemble of ejected stars, the Galactic center must have a significant population of young binary stars close enough to the central black hole.

Current observations provide broad support for many young stars at the Galactic center (e.g., Martins et al. 2005). Near Sgr A*, high spatial resolution observations reveal $\sim$100 or more young OB stars and many evolved Wolf-Rayet stars (Ghez et al. 2003; Schödel et al. 2003; Eisenhauer et al. 2005; Tanner et al. 2005; Paumard et al. 2006). Within 25–50 pc of Sgr A*, there are several distinct star-forming regions, including the Arches cluster, containing thousands of stars with masses $\gtrsim$3–4 $M_\odot$ (Figer et al. 1999; Najarro et al. 2004; Stolte et al. 2005). If the binary fraction of the OB population near the Galactic center is comparable to the local fraction of $\sim$70% (Kobulnicky et al. 2006), then the Galactic center contains enough binary stars to interact with the central black hole and to produce an observable population of HVSs.

The ejection rate from the central black hole depends on the structure of the inner Galaxy near Sgr A*. For a random phase-space distribution of binaries in the Galactic center, Hills (1988) first argued that the ejection rate could be as high as $\sim 10^{-2}$ yr^{-1}. Yu & Tremaine (2003) refined the calculation to account for the destruction of binaries whose orbits take them near Sgr A*. This

TABLE 3
MAXIMUM DISTANCE FROM THE GALACTIC CENTER AS A FUNCTION OF EJECTED MASS

m_1 ($M_\odot$)	t_{ms} (Myr)	m_2 ($M_\odot$)	a_{bin} (AU)	v_{ej} (km s^{-1})	d_{max} (kpc)
7.....	43	2	0.04	4500	193
	43	4	0.05	4400	184
	43	7	0.05	4800	200
9.....	26	2	0.05	4400	114
	26	4	0.06	4200	110
	26	9	0.06	4700	123
12.....	16	3	0.06	4400	71
	16	6	0.06	4700	76
	16	12	0.06	5200	83
15.....	12	4	0.06	4800	58
	12	8	0.07	4700	57
	12	15	0.07	5200	62
20.....	8	5	0.07	4800	39
	8	10	0.08	4800	39
	8	20	0.09	5035	41
30.....	5	8	0.10	4700	23
	5	15	0.11	4700	24
	5	30	0.12	5000	25

NOTES.—These columns list the average ejection velocity v_{ej} for the specified binary semimajor axis a_{bin} and the corresponding maximum galactocentric distance d_{max} that an ejected primary can achieve, as a function of the primary mass m_1 and the secondary mass m_2. Specifically, if the primary is ejected with velocity v_{ej}, d_{max} is the distance from the Galactic center the star reaches during its main-sequence lifetime t_{ms} as it travels radially outward through the Galactic halo. Here v_{ej} is taken from eq. (1) with $f_R = 1$, that is, assuming an optimal impact parameter R_{min}. The binary semimajor axis a_{bin} is chosen to reflect a minimum separation as a result of Roche lobe overflow. Note that it would be rare for a primary to actually achieve the listed d_{max}, since ejections are not common for very tight binaries.

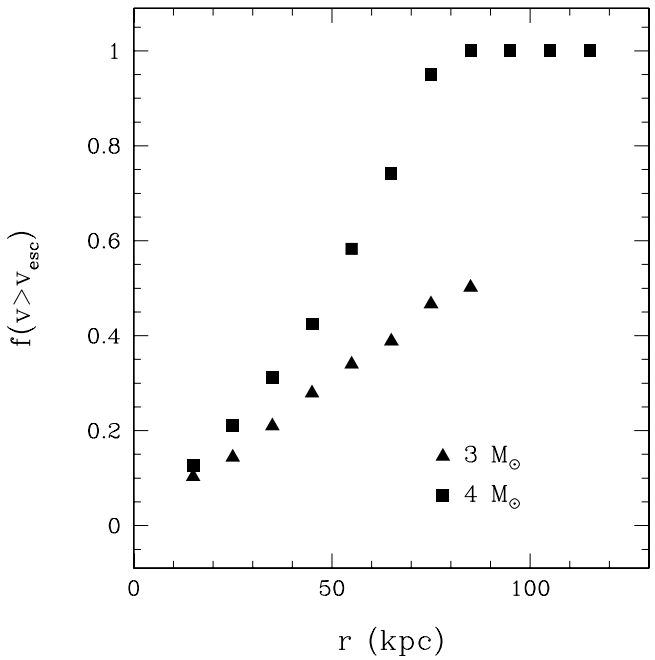

FIG. 5.—Fraction of observable ejected stars with radial velocities exceeding the escape velocity as a function of radial distance from the Galactic center. As indicated in the legend, squares show results for 4 $M_\odot$ primary stars; triangles show results for 3 $M_\odot$ primaries.

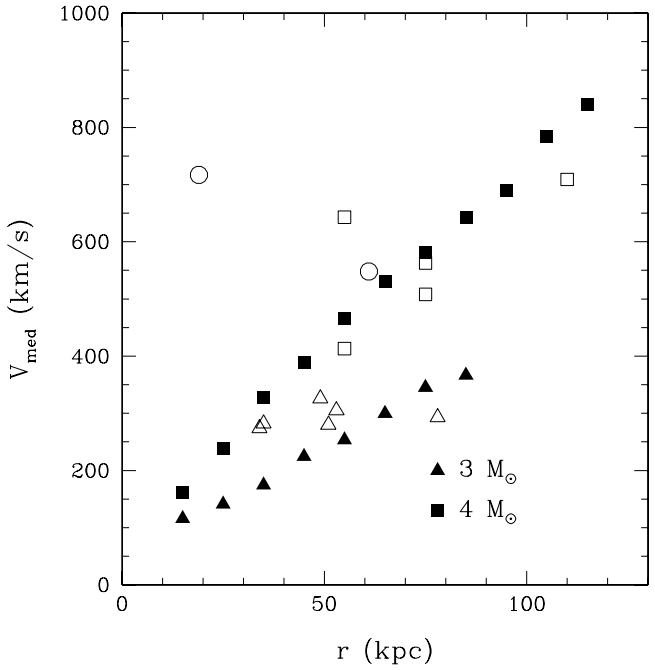

FIG. 6.—Median speeds of ejected 3 $M_\odot$ (*filled triangles*) and 4 $M_\odot$ (*filled squares*) primaries in the Galactic halo, as a function of distance from the Galactic center. In both cases the secondary mass is half that of the primary. The open squares represent the five HVSs discovered in a targeted survey (Brown et al. 2006b); the open triangles represent lower velocity, plausibly ejected, stars from this survey. The open circles represent two HVSs discovered independently (Edelmann et al. 2005; Hirsch et al. 2005), which are outside the mass range we consider.

region of phase space, the loss cone, is replenished by random scattering between binaries and other stars. If a steady state is reached, the ejection rate is $\sim 10^{-5}$ yr^{-1} for objects with binary separations within 0.3 AU. Recently, Perets et al. (2006) concluded that phase-space mixing by massive star clusters, molecular clouds, and perhaps intermediate-mass black holes produces a significantly larger ejection rate. They estimate a Galactic population of 10–200 HVSs with stellar masses of 4 $M_\odot$, consistent with observations (Brown et al. 2005, 2006a).

Once these ejected stars are in the halo, the velocity distributions derived from ongoing radial velocity surveys provide a test of the ejection model. To make a first comparison, we use data from the halo survey of Brown et al. (2006a, 2006b), and data for two HVSs from Edelmann et al. (2005) and Hirsch et al. (2005). The Brown et al. survey selects candidate B-type stars from the Sloan Digital Sky Survey (SDSS; Adelman-McCarthy et al. 2006) and derives distances, radial velocities, and spectral types from optical spectra acquired with the 6.5 m MMT. This survey is complete and can detect all B-type stars at any velocity out to $\sim$100–150 kpc. In addition to HVSs with radial velocities exceeding $\sim$400 km s^{-1}, Brown et al. (2006b) find an overabundance of B-type halo stars with radial velocities of $\sim$250–400 km s^{-1}. Because the observations show no evidence for an infalling population with comparable radial velocities, Brown et al. conclude that these outliers in the velocity distribution might be low-velocity HVSs or the high-velocity tail of runaway B-type stars (Portegies Zwart 2000).

To compare our predictions with the observations, Figure 6 shows the median radial velocity as a function of radial position in an $\alpha = 2.0$ model for 3 and 4 $M_\odot$ primaries with secondary star masses equal to half the primary mass. The radial variation in the median speed reflects the interdependence of the ejection velocity distribution, stellar lifetime, and survey volume. The trend toward higher median speed at larger distance results from the finite stellar lifetime of ejected stars; slow-moving stars cannot reach large distances within their main-sequence lifetimes (see also Baumgardt et al. 2006). With a sizable population of ejected star candidates, the velocity-radius relationship in this figure serves as a fundamental test of the stellar ejection hypothesis.

The comparison of the model prediction with observations of known high-velocity halo stars (Fig. 6, *open symbols*) is encouraging. In general, the model predicts roughly comparable numbers of HVSs and stars with radial velocities of 250–400 km s^{-1}, as observed in current surveys. Aside from the single subdwarf O-star outlier (Hirsch et al. 2005) at $r \sim 20$ kpc and $v_{med} \sim 700$ kms, the observed velocity distribution of HVSs also closely follows the predicted relation for 4 $M_\odot$ primary stars. The lone 8 $M_\odot$ HVS (Edelmann et al. 2005) at $r \sim 55$ kpc and $v_{med} \sim 550$ kms) lies within the group of lower mass B-type stars[2]. At lower velocities, the observed distribution lies between the predicted relations for 3 and 4 $M_\odot$ stars. With measured spectral types consistent with stellar masses of 3–4 $M_\odot$ for most HVSs and most of the low-velocity sample, we conclude that the observations are in excellent agreement with model predictions.

Although Galactic center ejections are necessary to explain the observed radial velocities above 400 km s^{-1}, objects with radial velocities of 250–400 km s^{-1} could be runaway B stars from supernova-disrupted binaries or other stellar dynamical interactions (e.g., Blaauw 1961; Poveda et al. 1967). However, for radial velocities exceeding $\sim$200 km s^{-1}, the velocity distribution of runaway stars should probably fall off more steeply than is observed (Leonard 1991; Portegies Zwart 2000). Current model predictions and statistics of halo stars with radial velocities of 250–400 km s^{-1} do not provide a conclusive test of the runaway B-star scenario. A simulation of the observable population of runaway B stars—similar in spirit to our simulation of the observable population of HVSs—would provide a good test of this mechanism.

Despite the small number of plausibly ejected stars in the sample of Brown et al. (2006b, 2006c), these objects provide an interesting test of models of the Galactic mass distribution. We consider the model with the steepest large-radius falloff in density, corresponding to $\alpha = 2.5$ in Table 1, and the HVSs listed by Brown et al. (2006b, their Table 1), shown here in Figure 6. None of the nine late-type B stars with distances in excess of 40 kpc from the Galactic center and speeds above 250 km s^{-1} have a speed in excess of the model's predicted median velocity of 752 km s^{-1}. Thus, we can rule out the model at a confidence level of 99.9%. If the objects with speeds less than 400 km s^{-1} are not ejected stars, then the confidence level drops to about 97%. Including the more massive early-type HVS (Edelmann et al. 2005), which should have a higher ejection speed than the late B-type stars, raises the confidence level above 98%. A similar argument using all 10 B stars suggests that the $\alpha = 2.2$ model is excluded with better than 98% confidence. The models with shallower large-radius falloff cannot be ruled out in this way.

These constraints on Galactic mass models depend heavily on the assumption that the known late-type HVSs have masses close to 4 $M_\odot$. If all objects were 3 $M_\odot$ stars, the predicted median velocity for ejected stars outside 30 kpc is 437 km s^{-1} in the $\alpha = 2.5$ model (Table 2). This median speed is consistent with the data. However, the model predicts that 25% of stars should have a speed greater than about 750 km s^{-1}. All 11 late-type

[2] We include the sdO star and the 8 $M_\odot$ B star for completeness. Our predicted distribution does not include massive B main-sequence stars or sdO stars.

B stars shown in Figure 6 have speeds in excess of 250 km s^{-1} and distances greater than 30 kpc, yet none has a speed exceeding 750 km s^{-1}. In this case, the $\alpha = 2.5$ model may be ruled out at the 95% confidence level; this level is even higher if we consider the early-type HSV as well. Note that these results depend mainly on the mass of the ejected primary, not on the mass of the secondary star (see Fig. 2).

In making these first probes of the Galactic mass distribution with HVSs, we note that larger samples of halo stars, globular clusters, and dwarf galaxies currently place better constraints on the mass distribution in the Galactic halo (e.g., Battaglia et al. 2005; Dehnen et al. 2006 and references therein). In particular, these data rule out the $\alpha \gtrsim 2.2$ models with higher significance than the known HVSs and lower velocity ejected stars. However, our results show that even small samples of HVSs are a potentially important probe of the Galactic mass distribution to large radii.

4. DISCUSSION AND SUMMARY

We have developed a first calculation of the predicted distribution of radial velocities for HVSs at galactocentric distances of 10–120 kpc in the Galactic halo. Our simulations quantify the ejection probabilities and velocities of binaries interacting with Sgr A*, generate the distribution of ejected stars from the vicinity of the Galactic center, and produce the full phase-space radial velocity distribution of ejected stars in the halo from an integration of the orbits of ejected stars through the Galactic potential. In addition to providing a framework for interpreting the observed velocity distribution of HVSs and related stars, the results of these simulations (Figs. 1–4) demonstrate that this approach can provide interesting constraints on the Galactic potential and on the mass function of the population of binary stars in the Galactic center.

Besides confirming the Hills (1988, 1992) results for the average velocity of ejected stars from the black hole, we derive a broad distribution of ejection velocities for each value of $a_{\rm bin}$ and $R_{\rm min}$. A Gaussian with $\sigma_v \sim 0.2 v_{\rm avg}$ provides a reasonable approximation to the derived velocity distribution. We plan to consider the origin of this distribution in future studies.

The initial comparisons between the model and observations are encouraging. The measured radial velocities of HVSs and stars with somewhat lower speeds agree well with the predictions. The current population of these stars provides a constraint on the Galactic mass distribution. As ongoing radial velocity surveys yield more HVSs with accurate stellar masses, the model will allow more robust tests for the origin of HVSs and lower velocity stars, will provide limits on the initial mass function of primary stars in the Galactic center, and will yield better constraints on mass models for the Galaxy.

As surveys reveal more HVSs, the observed velocity distribution of ejected stars in the Galactic halo may help to distinguish among alternative scenarios for producing HVSs. Compared to the single black hole models, binary black hole models produce relatively fewer ejections at the highest velocities (Yu & Tremaine 2003; Baumgardt et al. 2006). Although binary black hole models may yield larger ejection rates overall (e.g., Yu & Tremaine 2003), the two models produce similar velocity distributions at lower velocities. Thus, better constraints on the HVS distribution at the highest velocities may provide a test of the two pictures for HVS formation.

Refinements to the mass models can include more detailed Galactic structure, in particular, the Galactic disk. Indeed, Gnedin et al. (2005) have already proposed that HVSs can serve to probe halo triaxiality. Including the disk potential should lead to nonradial ejection velocities and may cause some clustering of ejected stars in the halo. We may therefore use the breakdown of spherical symmetry in the distribution of ejected stars about the Galactic center to reveal the Galaxy's structure.

If ejected stars are produced in short-lived star-forming regions near Sgr A* or if they originate in individual star clusters that settle dynamically into the Galactic center, ejected stars—including HVSs—may also cluster in time. Given a Galactic mass model, we can identify any temporal correlations by using the radial position and velocity of stars to determine the time since they were ejected. The extraction of temporal and spatial clustering information may be difficult with rare HVSs. However, a clustering analysis might be feasible with the more numerous, slower population of ejected stars suggested by our model.

We thank an anonymous referee for raising interesting issues that improved the paper. We acknowledge support from the NASA Astrophysics Theory Program through grant NAG5-13278.

REFERENCES

Abt, H. A. 1983, ARA&A, 21, 343
Adelman-McCarthy, J. K., et al. 2006, ApJS, 162, 38
Battaglia, G., et al. 2005, MNRAS, 364, 433
Baumgardt, H., Gualandris, A., & Portegies Zwart, S. 2006, MNRAS, 372, 174
Binney, J., & Tremaine, S. 1987, Galactic Dynamics (Princeton: Princeton Univ. Press)
Blaauw, A. 1961, Bull. Astron. Inst. Netherlands, 15, 265
Bromley, B. C., & Kenyon, S. J. 2006, AJ, 131, 2737
Brown, W. R., Geller, M. J., Kenyon, S. J., & Kurtz, M. J. 2005, ApJ, 622, L33
———. 2006a, ApJ, 640, L35
———. 2006b, ApJ, 647, 303
Brown, W. R., Geller, M. J., Kenyon, S. J., Kurtz, M. J. & Bromley, B. C. 2006c, ApJ, submitted
Dehnen, W., McLaughlin, D. E., & Sachania, J. 2006, MNRAS, 369, 1688
Duquennoy, A., & Mayor, M. 1991, A&A, 248, 485
Eckart, A., & Genzel, R. 1997, MNRAS, 284, 576
Edelmann, H., Napiwotzki, R., Heber, U., Christlieb, N., & Reimers, D. 2005, ApJ, 634, L181
Eggleton, P. P. 1983, ApJ, 268, 368
Eisenhauer, F., et al. 2005, ApJ, 628, 246
Figer, D. F., Kim, S. S., Morris, M., Serabyn, E., Rich, R. M., & McLean, I. S. 1999, ApJ, 525, 750
Garmany, C. D., Conti, P. S., & Massey, P. 1980, ApJ, 242, 1063
Ghez, A. M., Salim, S., Hornstein, S. D., Tanner, A., Lu, J. R., Morris, M., Becklin, E. E., & Duchêne, G. 2005, ApJ, 620, 744
Ghez, A. M., et al. 2003, ApJ, 586, L127
Ginsburg, I., & Loeb, A. 2006, MNRAS, 368, 221
Gnedin, O. Y., Gould, A., Miralda-Escudé, J., & Zentner, A. R. 2005, ApJ, 634, 344
Gould, A., & Quillen, A. C. 2003, ApJ, 592, 935
Gualandris, A., Portegies Zwart, S., & Sipior, M. S. 2005, MNRAS, 363, 223
Hansen, B. M. S., & Milosavljević, M. 2003, ApJ, 593, L77
Heacox, W. D. 1998, AJ, 115, 325
Hills, J. G. 1988, Nature, 331, 687
———. 1992, AJ, 103, 1955
Hirsch, H. A., Heber, U., O'Toole, S. J., & Bresolin, F. 2005, A&A, 444, L61
Hogg, D. W., Blanton, M. R., Roweis, S. T., & Johnston, K. V. 2005, ApJ, 629, 268
Holley-Bockelmann, K., Sigurdsson, S., Mihos, J. C., Feldmeier, J. J., Ciardullo, R., & McBride, C. 2005, ApJL, submitted (astro-ph/0512344)
Kenyon, S. J., & Bromley, B. C. 2006, AJ, 131, 1837
Kobulnicky, H. A., Fryer, C. L., & Kiminki, D. C. 2006, ApJ, submitted (astro-ph/0605069)
Leonard, P. J. T. 1991, AJ, 101, 562

Levin, Y., Wu, A., & Thommes, E. 2005, ApJ, 635, 341
Martins, F., Genzel, R., Paumard, T., Abuter, R., Eisenhauer, F., Gillessen, S., Ott, T., & Trippe, S. 2005, in SF2A-2005: Semaine de l'Astrophysique Francaise, ed. F. Casoli et al. (Strasbourg: EdP-Sciences), 581
Najarro, F., Figer, D. F., Hillier, D. J., & Kudritzki, R. P. 2004, ApJ, 611, L105
Paumard, T., et al. 2006, ApJ, 643, 1011
Perets, H. B., Hopman, C., & Alexander, T. 2006, ApJ, submitted (astro-ph/0606443)
Portegies Zwart, S. F. 2000, ApJ, 544, 437
Poveda, A., Ruiz, J., & Allen, C. 1967, Bol. Obs. Tonantzintla Tacubaya, 4, 86
Quinlan, G. D. 1996, NewA, 1, 35
Schaerer, D., Charbonnel, C., Meynet, G., Maeder, A., & Schaller, G. 1993, A&AS, 102, 339
Schaller, G., Schaerer, D., Meynet, G., & Maeder, A. 1992, A&AS, 96, 269
Schödel, R., Ott, T., Genzel, R., Eckart, A., Mouawad, N., & Alexander, T. 2003, ApJ, 596, 1015
Sesana, A., Haardt, F., & Madau, P. 2006, ApJ, 651, 392
Stolte, A., Brandner, W., Grebel, E. K., Lenzen, R., & Lagrange, A.-M. 2005, ApJ, 628, L113
Tanner, A., Ghez, A. M., Morris, M. R., & Christou, J. C. 2005, ApJ, 624, 742
Yoshida, H. 1990, Phys. Lett. A, 150, 262
Yu, Q. 2002, MNRAS, 331, 935
Yu, Q., & Tremaine, S. 2003, ApJ, 599, 1129